Low-loss silicon-on-insulator shallow-ridge TE and TM waveguides formed using thermal oxidation

R. Pafchek,[1] R. Tummidi,[1] J. Li,[1,2] M. A. Webster,[1,3] E. Chen,[4] and T. L. Koch[1,*]

[1]Center for Optical Technologies, Lehigh University, Bethlehem, Pennsylvania 18015, USA

[2]Currently at Sun Microsystems Inc., 9525 Towne Centre Drive, San Diego, California 92121, USA

[3]Currently at Lightwire Inc., 7540 Windsor Drive, Allentown, Pennsylvania 18195, USA

[4]Bell Laboratories, Alcatel-Lucent, 600 Mountain Avenue, Murray Hill, New Jersey 07974, USA

*Corresponding author: tlkoch@Lehigh.edu

Received 10 July 2008; revised 7 January 2009; accepted 9 January 2009;
posted 12 January 2009 (Doc. ID 98678); published 4 February 2009

A thermal oxidation fabrication technique is employed to form low-loss high-index-contrast silicon shallow-ridge waveguides in silicon-on-insulator (SOI) with maximally tight vertical confinement. Drop-port responses from weakly coupled ring resonators demonstrate propagation losses below 0.36 dB/cm for TE modes. This technique is also combined with "magic width" designs mitigating severe lateral radiation leakage for TM modes to achieve propagation loss values of 0.94 dB/cm. We discuss the fabrication process utilized to form these low-loss waveguides and implications for sensor devices in particular.

OCIS codes: 130.0130, 130.3120, 130.3130, 130.2790, 130.5990.

1. Introduction

Silicon photonics is gaining increased interest for a broad spectrum of applications, with advantages including a low-cost and robust materials system, the ability to leverage highly advanced CMOS processing infrastructure, and the potential for compatibility with on-chip electronics. Recently Densmore *et al.* [1] showed that high-index-contrast systems operating in the TM mode are ideally suited for interferometric sensors that rely on perturbations in the modal effective index caused by the interaction of the evanescent tail of the mode with solutions or material adsorbed on the waveguide surface. In particular, silicon-on-insulator (SOI) is shown to provide order-of-magnitude increases in sensitivity compared to other material systems.

Sensitivity of evanescent-wave surface sensors depends critically on maximizing field overlap with the adsorbed species, but precision in phase measurement also requires long interaction lengths in either a long interferometric configuration or a high-Q resonator, so waveguide propagation losses will also impose a limit on the sensitivity. Thin-core shallow-ridge waveguides can potentially optimize both these attributes. However, it is well known that waveguide scattering losses, which can be shown to scale as $(\Delta n)^2$ through analytical means [2], are exacerbated in tight vertical confinement SOI guides due both to the high index contrast and the higher modal amplitude at the interfaces with the low-index cladding or sensing layers. Reactive ion etching (RIE) is typically used to pattern Si-core SOI waveguides and significant (multinanometer scale) sidewall roughness is commonly encountered from standard lithographic and etching processes. This suggests alternative fabrication techniques for highly smooth waveguides that also minimize exposure of the mode to etched interfaces. Finally, the desired TM-mode operation in shallow-ridge waveguides can also lead to inherent severe lateral radiation leakage loss in high-index-contrast systems. This leakage can be eliminated by etching the ridge with sufficient depth such

0003-6935/09/050958-06$15.00/0

that the two-dimensional TE mode for a slab with a thickness corresponding to the resulting thin lateral ridge cladding region has a lower effective index than the full three-dimensional TM mode of the ridge waveguide. However, this approach can be problematic since a sufficiently deep ridge presents a much larger rough scattering interface, leading to higher losses, and can also make electrical access for active devices problematic. We have recently demonstrated the effectiveness of "magic width" designs in mitigating lateral leakage losses [3]. This effect can be shown to result from destructive interference of radiation loss components that are generated when light in the core impinges on the lateral step boundaries on each side of the ridge.

We show that smooth surfaces can be achieved by replacing the RIE etching step with a thermal oxidation process. We demonstrate nearly maximally confined waveguides with losses below 0.36 dB/cm for TE modes corresponding to measured resonator Q values of 1.6×10^6. For high sensitivity in sensor applications, we then combine this waveguide fabrication technique with "magic width" designs to mitigate TM lateral leakage losses and achieve 0.94 dB/cm for TM modes, corresponding to resonator Q values of 6.8×10^5. This waveguide design and fabrication technique should offer nearly ideal performance in interferometric or resonator-based sensor configurations.

2. Waveguide Design

As noted in Section 1, the sensitivity of evanescent-wave sensors for surface adsorbed species can be strongly enhanced by increasing the magnitude of the modal electric field at the waveguide surface. The change in modal effective index is given by the well-known expression [4]

$$\Delta n_{\text{eff}} = \frac{c\varepsilon_o \int_{-\infty}^{\infty} \Delta(n^2(x))\mathbf{E}\cdot\mathbf{E}^* \mathrm{d}x}{\int_{-\infty}^{\infty}(\mathbf{E}\times\mathbf{H}^* + \mathbf{E}^*\times\mathbf{H})\cdot\hat{\mathbf{z}}\mathrm{d}x}, \tag{1}$$

where $n(x)$ is the index of refraction profile, c is the speed of light, ε_0 is the permittivity of free space, and $\mathbf{E}$ and $\mathbf{H}$ are the electric and magnetic fields. This expression has substantially different behavior for TE and TM modes. For TE modes, the boundary conditions on the parallel upper waveguide interface ensure that the electric field, while large due to tight confinement, is continuous across the waveguide upper surface. In the case of TM, however, the magnetic field is continuous and the normal component of the displacement is continuous, requiring that the (predominant) normal electric field jumps by a ratio of $n^2_{\text{core}}/n^2_{\text{surface}}$ for the surface layer. As a result, changes in effective index due to index changes on the upper surface of the Si waveguide core are maximized with thin, high-index contrast guides and TM polarization. Using the expression above and the approximation $\Delta(n^2) \cong 2n\cdot\Delta n$, we can plot the normalized integrand in Eq. (1) as a "weighting function" $f(x)$ to illustrate the sensitivity of changes in modal effective index to changes in the index $\Delta n(x)$ in any portion of a waveguide structure:

$$\Delta n_{\text{eff}} = \int_{-\infty}^{\infty} \Delta n(x)\cdot f(x)\mathrm{d}x, \tag{2}$$

where the weighting function $f(x)$ is given by

$$f(x) = \frac{2c\varepsilon_o n(x)\mathbf{E}\cdot\mathbf{E}^*}{\int_{-\infty}^{\infty}(\mathbf{E}\times\mathbf{H}^* + \mathbf{E}^*\times\mathbf{H})\cdot\hat{\mathbf{z}}\mathrm{d}x}. \tag{3}$$

This weighting function is illustrated in Fig. 1 for a slab SOI waveguide with a 205 nm Si device layer thickness and a thick buried oxide (BOX) layer with water as the upper cladding. As can be seen from Fig. 1, operation in the TM mode provides significant enhancement in sensitivity at the waveguide surface in the low-index cladding medium. While it is evident from this figure, it is also straightforward to show, through a rigorous nonperturbative numerical analysis, that the sensitivity of index change of the TM mode to molecules adsorbed on the surface in nanometer-scale layers is ~4.3 times more than that obtained in TE-mode operation. Similarly, using either the weighting function or rigorous nonperturbative analysis, it is easy to illustrate the dependence of evanescent-wave sensor effective index change on waveguide core thickness, as shown in Fig. 2. This figure demonstrates that the optimum core thickness for peak TM sensitivity to nanometer-scale surface index changes for a slab SOI guide clad with water

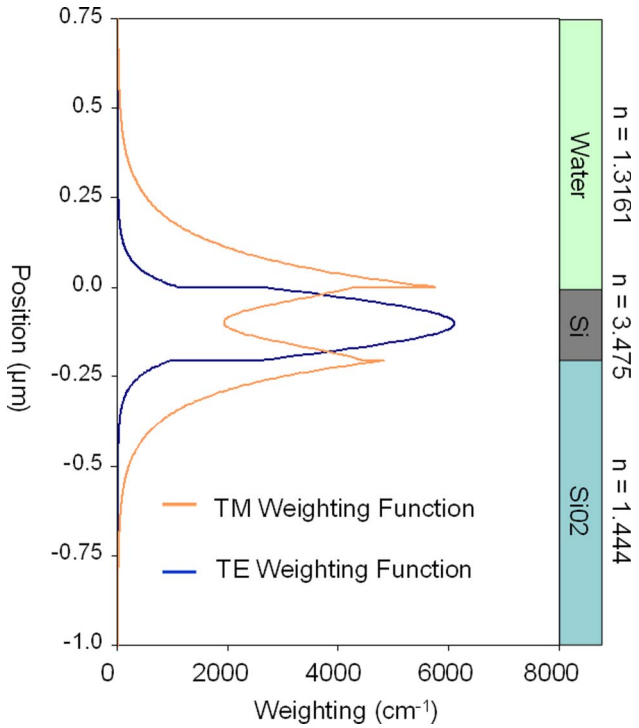

Fig. 1. (Color online) Weighting function for TE and TM modes for a 205 nm slab SOI guide with H_2O upper cladding.

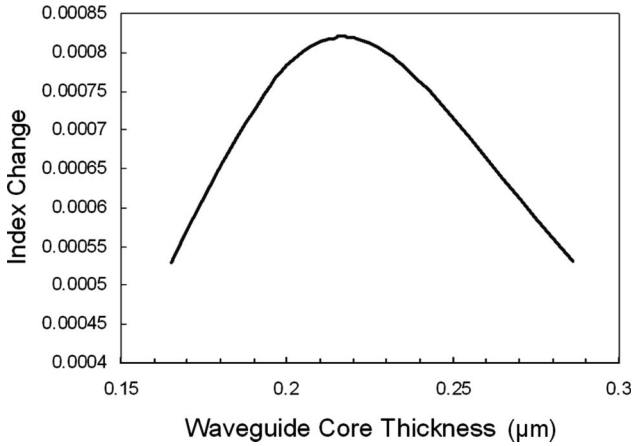

Fig. 2. Dependence of TM modal effective index change on silicon core thickness for the slab waveguide system described in Fig. 1 when an additional 1 nm thick layer of material with index $n = 1.5$ is deposited on upper core surface.

on the upper surface is ~208 nm. The guides used in our experiment are illustrated in Fig. 3, and the 205 nm core thickness used in our experiments is very close to the optimum value, incurring $<2\%$ reduction in sensitivity relative to the best value.

While the TM mode provides enhanced sensitivity, mitigation of the TM-mode lateral radiation leakage loss into slab TE modes requires design at "magic widths." These widths can be analytically computed using [3]

$$W_{\text{magic}} = M \cdot \lambda \cdot (n^2_{\text{TE-slab-core}} - N^2_{\text{eff-TM}})^{-\frac{1}{2}} \quad \text{for } M = 1, 2, 3, \ldots, \tag{4}$$

where $n_{\text{TE-slab-core}}$ is the two-dimensional (slab) effective index of the TE mode in the core, while $N_{\text{eff-TM}}$ is the full three-dimensional effective index of the TM quasi-mode for the structure. Since the later depends weakly on the waveguide width W, Eq. (1) can easily be solved iteratively. Finally, it is important to have sufficient BOX layer thickness to avoid radiation loss to the silicon substrate. For BOX thicknesses of $2\,\mu$m or greater in the guide structure illustrated in Fig. 3, substrate radiation loss is computed to be <0.01 dB/cm for TM modes and well below this value for TE modes.

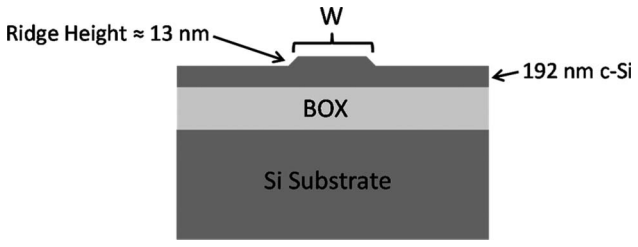

Fig. 3. Quasi-planar ridge SOI waveguide geometry. BOX thickness is $2\,\mu$m.

3. Waveguide Fabrication and Experiment

Soitec SOI substrates were used to fabricate the ridge waveguides. The silicon device layer in the SOI wafers is 205 nm thick with a $2\,\mu$m BOX layer underneath. To minimize any sidewall roughness, the ridges were formed via an ultrasmooth thermal oxidation process [5]. Figure 4 gives a process flow chart illustrating the fabrication sequence we employed in this experiment. To form a waveguide structure with this technique an appropriate masking material, such as Si_3N_4, is advantageous because oxygen diffusion through the nitride layer is negligible, thereby protecting the silicon underneath. A patterned nitride layer can thus serve as a mask during a high-temperature oxygen annealing process. This technique not only minimizes side-wall roughness, but also has the advantage of providing high uniformity across the wafer. Furthermore, if an oxide film or some other semipermeable layer is incorporated between the Si and nitride, the resulting waveguide profile can be optimized for a given application by adjusting the oxide layer thickness in order to control the oxygen diffusion through this layer near the ridge sidewalls. As has been discussed previously [6], optical losses are also minimized in this design by the reduced etch depth into the silicon device layer associated with the ridge waveguide as compared to wire waveguides, where the silicon device layer is fully etched. This is accomplished simply by controlling the oxidation time, which gives a highly precise control on the height on the waveguide ridges compared to traditional etching processes. By reducing the waveguide optical loss, longer propagation lengths or higher-Q resonators can be employed in sensor configurations, as discussed in Section 1, enabling enhanced performance for evanescent-wave sensors.

The detailed fabrication process for the ridge waveguide formation started with the deposition of a 100 nm plasma-enhanced chemical vapor deposition (PECVD) SiO_2 followed by a 25 nm thick PECVD Si_3N_4 layer. A $1\,\mu$m thick AZ703 resist was spin coated onto the wafer and exposed with a projection printer. A 6:1 ammonium fluoride:hydrofluoric acid solution was used to transfer the pattern into the

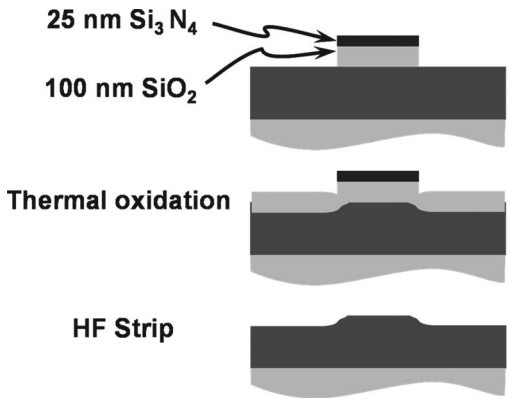

Fig. 4. Processing steps for ridge waveguide fabrication.

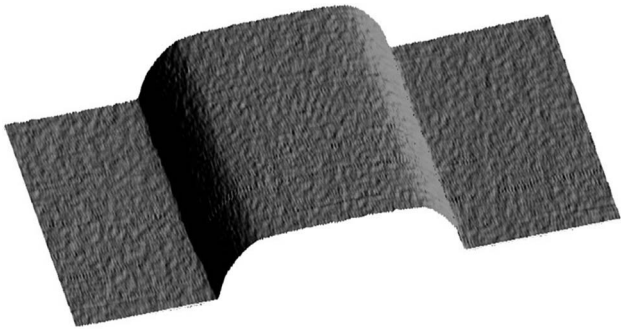

Fig. 5. AFM trace of a 1.44 μm ridge waveguide displaying $<$0.2 nm surface roughness.

nitride/oxide layers. Once the pattern was formed, the resist was stripped and the resulting structure was then oxidized at 975 °C in O_2 for 17 min to form 13 nm ridges. The residual mask and the thermally formed SiO_2 were then stripped with HF, resulting in a waveguide structure with very smooth silicon surface and side wall, as shown in the atomic force microscope (AFM) trace in Fig. 5. The RMS surface roughness was measured to be less than 0.2 nm, which is an order of magnitude less than that typically obtained with conventional etching processes. After the ridge waveguides were formed with the process described above, a layer of resist was applied to protect the surface during dicing and end facet polishing of the resulting chips. Finally, the protective resist layer was removed from the finished chips using acetone and alcohol.

To accurately quantify the losses of our waveguides, we use the resonance characteristics of undercoupled ring resonators [7,8]. Figure 6 shows the schematic of the ring resonator circuit formed using the ridge waveguides described above and the full width at half-maximum (FWHM) of the resonance linewidth $\Delta\nu$ as measured through the drop port. The configuration in Fig. 6(a) has separate through and drop ports and consists of two directional couplers that are designed to be undercoupled relative to the waveguide losses in the ring resonator. In this ring resonator configuration the FWHM of the drop-port response $\Delta\omega$ is related to the effective intensity attenuation coefficient α_{rt} for one round trip according to

$$\Delta\omega = \alpha_{\mathrm{rt}} v_g, \tag{5}$$

where v_g is the group velocity. The round-trip loss α_{rt} is the sum of the waveguide propagation losses α and the coupling losses from the two directional couplers (α_1 and α_2) but, if the ring is designed is to be weakly coupled, then $\Delta\omega \approx \alpha v_g$. Since precision frequency scans allow for an accurate determination of resonance width, this provides an unambiguous and conservative figure for waveguide losses. If desired, the weak contributions from coupler losses can be removed for a correction.

Loss measurements were conducted using an external cavity laser diode with a linewidth of $<$10 MHz and a continuous single-longitudinal mode very fine-tuning capability. The laser output was first fed through a polarization controller and tapered fibers with six-axis piezo-controlled translation stages were used to couple the signal into and out of the waveguide ports. The output from the waveguide was detected by a power meter, followed by analog-to-digital conversion allowing computerized data collection. The shape of the resonance profile is recorded by scanning the laser across the resonance peaks, as shown in Fig. 6(b), allowing for the determination of the FWHM linewidths and corresponding resonator losses.

4. Results and Discussion

Figure 7 shows the average TE and TM drop-port response for a 400 μm radius ring resonator with a waveguide "magic width" of 1.44 μm in the ring as well as in the straight waveguides and couplers. Both of these responses were obtained on the same device. While the waveguides have very strong birefringence, with calculated phase index values of $n_{\mathrm{TE}} = 2.768$ and $n_{\mathrm{TM}} = 1.740$, the group index values are nearly identical due almost entirely to the strong structural waveguide dispersion. The measured group index values were $n_{g\text{-TE}} = 3.721$ and $n_{g\text{-TM}} = 3.847$ for the TE and TM modes, respectively, as determined from the free spectral range of the resonators, and agree fairly well with calculated values including several percent corrections from silicon material dispersion. Using these measured group index values, the measured linewidths of $\Delta\nu_{\mathrm{FWHM\text{-}TE}} = 124.37$ MHz and $\Delta\nu_{\mathrm{FWHM\text{-}TM}} = 286.33$ MHz correspond to losses of 0.42 dB/cm and

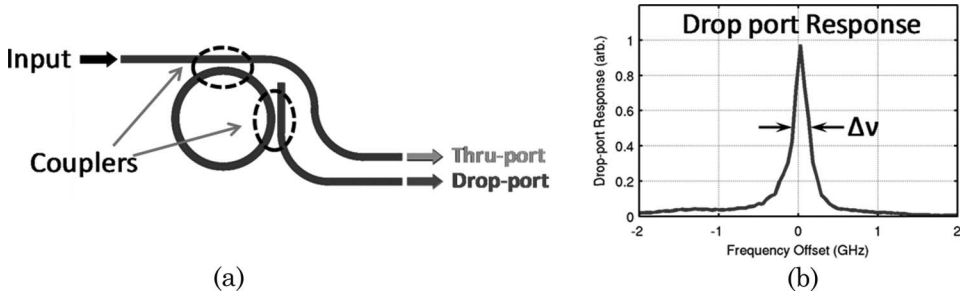

(a) (b)

Fig. 6. (a) Ring resonator with add-drop ports and (b) an exemplary drop-port response.

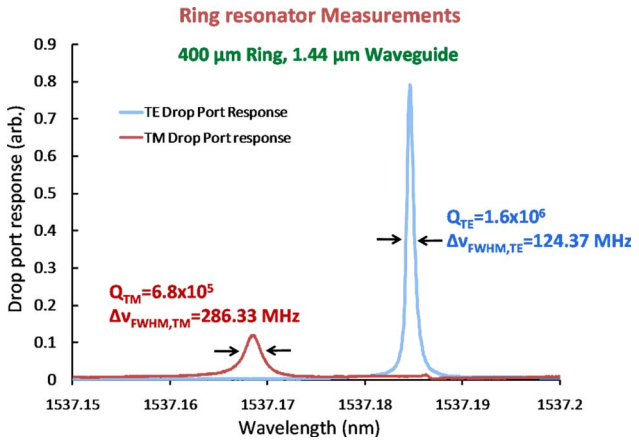

Fig. 7. (Color online) Drop-port responses for the TE and TM modes for a 400 μm radius ring resonator with "magic width" waveguide of 1.44 μm.

1.00 dB/cm and for the TE and the TM modes, respectively. As noted in Section 3, this provides a conservative figure because all loss is ascribed to propagation. Conventional bending losses are readily estimated analytically and, for the waveguide design used in this experiment, are calculated to be $<$0.03 dB/cm for TE modes and orders of magnitude smaller for TM modes and have been, therefore, neglected. The couplers in the device are fabricated with a straight waveguide running tangentially by the ring with the gap between the edges of the ridge at the closest point of 1.87 μm. The coupling coefficient for this design was evaluated using the two-dimensional BeamPROP program [9], which yielded a coupling coefficient of 0.18% for the TE mode and 0.19% for the TM mode per coupler. Using these computed values, a correction can be included for the two couplers combined, with a contributed loss of 0.062 dB/cm for the TE mode and 0.066 dB/cm for the TM mode. This results in waveguide propagation losses of 0.36 dB/cm and 0.94 dB/cm and for the TE and TM modes, respectively.

A variation in the loss values with wavelength for the TM mode was observed as expected due to the "magic width" effect. Since the actual fabricated width may not precisely correspond to the "magic width", the wavelength was tuned in these measurements in order to minimize the FWHM of the drop-port responses and the minima were obtained at 1537 nm. We also saw small variations of successive resonances exhibiting $\pm$10% differences in the peak widths about the average loss values quoted above which might be defect related and are under investigation. Additionally, while the TM loss is quite low, it is not as low as the TE loss even at the "magic width" values. This additional loss may be due to additional anomalous radiation losses resulting form imperfect radiation cancellation in curved waveguides even at "magic widths" and is under investigation.

The corresponding Q values for these ring resonators are 1.6×10^6 and 6.8×10^5 and for TE and TM, respectively. To our knowledge, these are the lowest published loss values for TE- and TM-mode SOI waveguides with ultrahigh vertical confinement designs suitable for optimized sensors. The very sharp resonance peaks arising from very low transmission losses in these waveguides can be utilized as a means of sensing biological or chemical agents adhering on a functionalized waveguide surface [8]. Because of the significant refractive index temperature dependence of silicon, thermal stability may be a significant performance issue in utilizing a ring resonator approach. Alternatively, a Mach–Zehnder device configuration designed with folded centimeter-scale path lengths that correspond to the effective total circulation path in the ring, $L_{\text{eff}} \approx \alpha^{-1}$, ideally can result in no reduction in sensitivity and may offer a preferred approach. Using the low-loss waveguides demonstrated in this paper, combined with the favorably low bending loss of TM modes, compactly folded designs should be readily achievable with little excess loss.

5. Conclusions

We have demonstrated a thermal oxidation fabrication technique producing silicon ridge waveguides on SOI with propagation losses of 0.36 dB/cm for TE modes. Combining the process with the "magic width" design criteria has also allowed us to achieve 0.94 dB/cm for the TM mode in a near-maximal vertical confinement 205 nm core thickness SOI waveguide. To our knowledge, these are the lowest losses for ultratight vertical confinement SOI waveguides reported to date, and should provide a means to achieve ultra-high-sensitivity surface evanescent-wave detection for biological and chemical species.

The authors gratefully acknowledge support from the United States Air Force Office of Scientific Research Multidisciplinary University Research Initiative (US AFOSR MURI) on Electrically-Pumped Silicon-Based Lasers for Chip-Scale Interconnects under Gernot Pomrenke, the commonwealth of Pennsylvania under Ben Franklin Technology Development Authority (BFTDA) grant ME#21-116-0014, the United States Army Research Laboratory (US ARL) under cooperative agreement W911NF-04-2-0015, and the support and encouragement of Alice E. White and Sanjay Patel of Alcatel-Lucent Bell Laboratories.

References

1. A. Densmore, D. X. Xu, P. Waldron, S. Janz, P. Cheben, J. Lapointe, A. Delge, B. Lamontagne, J. H. Schmid, and E. Post, "A silicon-on-insulator photonic wire based evanescent field sensor," IEEE Photon. Technol. Lett. **18**, 2520–2522 (2006).
2. J. P. R. Lacey and F. P. Payne, "Radiation loss from planar waveguides with random wall imperfections," IEE Proc. Optoelectron. **137**, 282–288 (1990).
3. M. A. Webster, R. M. Pafchek, A. Mitchell, and T. L. Koch, "Width dependence of inherent TM-mode lateral leakage loss in silicon-on-insulator ridge waveguides," IEEE Photon. Technol. Lett. **19**, 429–431 (2007).

4. H. Kogelnik, "Theory of optical waveguides," in *Guided-Wave Optoelectronics*, T. Tamir, ed. (Springer Verlag, 1990), pp. 7–87.
5. T. L. Koch, R. M. Pafchek, and M. A. Webster, "Fabrication of optical waveguides," U.S. patent application 20060098928 (11 May 2006).
6. A. Ksendzov and Y. Lin, "Integrated optics ring-resonator sensors for protein detection," Opt. Lett. **30**, 3344–3346 (2005).
7. M. A. Webster, R. M. Pafchek, G. Sukumaran, and T. L. Koch, "Low-loss quasi-planar ridge waveguides formed on thin silicon-on-insulator," Appl. Phys. Lett. **87**, 231108 (2005).
8. D. K. Armani, T. J. Kippenberg, S. M. Spillane, and K. J. Vahala, "Ultra-high-*Q* toroid microcavity on a chip, " Nature **421**, 925–928 (2003).
9. Rsoft Design Group, Inc., 400 Executive Boulevard, Suite 100, Ossining, N.Y. 10562, USA, www.rsoftdesign.com.